The *Xanthomonas* type III effector XopAP prevents stomatal closure by interfering with vacuolar acidification[oo]

Longyu Liu[1,2], Ying Li[1], Zhengyin Xu[1], Huan Chen[2,3], Jingyi Zhang[2,3], Brittany Manion[2], Fengquan Liu[3], Lifang Zou[1], Zheng Qing Fu[2*] and Gongyou Chen[1*]

1. State Key Laboratory of Microbial Metabolism/Shanghai Collaborative Innovation Center of Agri-Seeds, School of Agriculture and Biology, Shanghai Jiao Tong University, Shanghai 200240, China
2. Department of Biological Sciences, University of South Carolina, Columbia 29208, USA
3. Institute of Plant Protection, Jiangsu Academy of Agricultural Sciences, Nanjing 210014, China

*Correspondences: Gongyou Chen (gyouchen@sjtu.edu.cn, Dr. Chen is fully responsible for the distribution of the materials associated with this article); Zheng Qing Fu (zfu@mailbox.sc.edu)

Longyu Liu   **Gongyou Chen**

ABSTRACT

Plant stomata close rapidly in response to a rise in the plant hormone abscisic acid (ABA) or salicylic acid (SA) and after recognition of pathogen-associated molecular patterns (PAMPs). Stomatal closure is the result of vacuolar convolution, ion efflux, and changes in turgor pressure in guard cells. Phytopathogenic bacteria secrete type III effectors (T3Es) that interfere with plant defense mechanisms, causing severe plant disease symptoms. Here, we show that the virulence and infection of *Xanthomonas oryzae* pv. *oryzicola* (*Xoc*), which is the causal agent of rice bacterial leaf streak disease, drastically increased in transgenic rice (*Oryza sativa* L.) plants overexpressing the *Xoc* T3E gene *XopAP*, which encodes a protein annotated as a lipase. We discovered that XopAP binds to phosphatidylinositol 3,5-bisphosphate (PtdIns(3,5)P_2), a membrane phospholipid that functions in pH control in lysosomes, membrane dynamics, and protein trafficking. XopAP inhibited the acidification of vacuoles by competing with vacuolar H^+-pyrophosphatase (V-PPase) for binding to PtdIns(3,5)P_2, leading to stomatal opening. Transgenic rice overexpressing *XopAP* also showed inhibition of stomatal closure when challenged by *Xoc* infection and treatment with the PAMP flg22. Moreover, XopAP suppressed flg22-induced gene expression, reactive oxygen species burst and callose deposition in host plants, demonstrating that XopAP subverts PAMP-triggered immunity during *Xoc* infection. Taken together, these findings demonstrate that XopAP overcomes stomatal immunity in plants by binding to lipids.

INTRODUCTION

Rice (*Oryza sativa* L.) is an important food crop for more than half of the world's population and has been cultivated for over 10 000 years (Khush, 2005). *Xanthomonas oryzae* pv. *oryzicola* (*Xoc*) causes bacterial leaf streak (BLS) in rice (Fang et al., 1957; Swings et al., 1990), which is considered one of the most serious diseases that can infect this crop species (Niño-Liu et al., 2006; Zou et al., 2006, 2011; Ji et al., 2016; Xu et al., 2021). The pathogen enters through leaf

stomata and colonizes the parenchyma apoplast to develop interveinal lesions that initially appear water-soaked before developing into translucent and yellow-to-white streaks (Swings et al., 1990). Thus, studying how the pathogen infects rice via stomata is essential to our understanding how plant pathogens in general, and *Xoc* in particular, cause diseases (Hu et al., 2022).

Type III effectors (T3Es) have been demonstrated to interfere with the assembly of the cytoskeleton, mitogen-activated protein kinase cascades, gene expression, proteasome-dependent protein degradation, and phytohormone signaling pathways to facilitate invasion by pathogenic bacteria (Büttner, 2016). Stomata are the principal entry sites through which plant pathogenic bacteria invade the intracellular leaf space (Lawson and Blatt, 2014). As a counteracting measure, guard cells initiate an innate immune response by reducing their cellular turgor pressure, which promotes stomatal closure once a microbial pathogen is recognized (McLachlan et al., 2014; Ye and Murata, 2016). Calcium influx is one of the early cellular events triggered by pathogen-associated molecular patterns (PAMPs) and occurs within 30 sec of microbial pattern perception. Ca^{2+} influx can control stomatal closure, thereby protecting plants from pathogen invasion through stomata (Margets et al., 2021). The genes encoding the HYPEROSMOLALITY-GATED Ca^{2+}-PERMEABLE CHANNELS1.3/1.7 (OSCA1.3 and OSCA1.7), which are phosphorylated by BOTRYTIS-INDUCED KINASE1 (BIK1) to activate the Ca^{2+} channels to induce pattern-induced stomatal immunity, are extensively expressed in guard cells (Thor et al., 2020). The outflow of anions from guard cells is involved in PAMP-induced stomatal closure, leading to immunity (Guzel Deger et al., 2015).

Many Gram-negative animal and plant pathogenic bacteria use a type III secretion system (T3SS) to deliver T3Es into their host cells (Notti and Stebbins, 2016). These T3Es suppress host defenses and allow infection. To block stomatal immunity, plant pathogenic bacteria may release T3Es and phytotoxins to suppress stomatal closure. Coronatine (COR) is a polyketide toxin formed by amide bonds linking coronamic acid (CMA) and coronafacic acid (CFA) (Ichihara et al., 1977). COR reopens plant stomata depending on the CORONATINE INSENSITIVE1 (COI1) (Melotto et al., 2006) and is essential for full virulence of *Pseudomonas syringae* pv. *tomato* (*Pst*) DC3000 (Brooks et al., 2004). Notably, the kinase T3E XopC2 from *Xoc* RS105 phosphorylates ORYZA SATIVA SKP1-LIKE PROTEIN1 (OSK1) for degradation of JASMONATE-ZIM-DOMAIN PROTEIN (JAZ) transcriptional repressors to suppress stomatal immunity in rice (Wang et al., 2021). The *P. syringae* T3E AvrE was recently reported to target type one protein phosphatases to disrupt the abscisic acid (ABA) signaling pathway and cause stomatal closure, resulting in an aqueous environment for infection (Hu et al., 2022).

The acidification of vacuoles mediated by phosphatidylinositol-3,5-bisphosphate (PtdIns(3,5)P$_2$) is thought to play important roles in stomatal closure. In eukaryotic cells, PtdIns(3,5)P$_2$ is a signaling lipid present in endo-lysosomal and vacuolar membranes (Carpaneto et al., 2017). Tonoplast-associated PtdIns(3,5)P$_2$ was proposed to be a regulator of vacuolar morphology (Gerth et al., 2017). The inhibition of PtdIns(3,5)P$_2$ biosynthesis results in diminished vacuole-luminal acidification during ABA-induced stomatal closure in broad bean (*Vicia faba*) plants (Bak et al., 2013). The function of vacuolar H$^+$-adenosine triphosphatases (VHA) such as VHA1 and VHA2 may be dependent on the biosynthesis of PtdIns(3,5)P$_2$. The *sac2 sac3 sac4 sac5* (*suppressor of actin*) quadruple mutant in *Arabidopsis thaliana*, which is defective in phosphoinositide phosphatase activity, showed slightly increased PtdIns(3,5)P$_2$ levels and a more tubular vacuolar morphology than wild-type plants, while vacuolar coalescence was enhanced in plants overexpressing *SAC2* or *SAC5* (Nováková et al., 2014). PtdIns(3,5)P$_2$ alters vacuolar pH by directly regulating vacuolar-type adenosine triphosphatase (V-ATPase) activity (Li et al., 2014). However, it has not been reported that any T3E targets PtdIns(3,5)P$_2$ to induce stomata closures for successful infection of plants by pathogens.

XopAP, which is a T3E protein of *Xoc*, is annotated as a lipase (Bogdanove et al., 2011). Lipases, a subclass of esterases, are water-soluble enzymes that catalyze the hydrolysis of ester bonds in lipids, converting triglycerides into glycerol and fatty acids (Joyce et al., 2016). However, few lipases from plant pathogens have been functionally characterized. The *Pseudomonas aeruginosa* T3E ExoU, which is cytotoxic to yeast (*Saccharomyces cerevisiae*), is a lipase (Sato et al., 2003). The lipase inhibitors iPLA2 and cPLA2 reduce the cytotoxicity of ExoU. ExoU resulted in lower levels of radiolabeled neutral lipids and the accumulation of free palmitic acid in yeast by thin-layer chromatography. The lipase activity of the effector *Fusarium graminearum* lipase1 (FGL1) is required for full virulence of the plant fungal pathogen *F. graminearum* (Blümke et al., 2014). Further results showed that FGL1 suppresses callose deposition by releasing the polyunsaturated free fatty acids linoleic and α-linolenic acid.

In this study, we focused on the *Xoc* T3E XopAP, which has a lipase domain. However, despite multiple attempts using different methods, no lipase activity has been detected for this protein. Instead, we demonstrate here that XopAP binds to PtdIns(3,5)P$_2$, a phosphorylated phosphatidylinositol that regulates the pH of some organelles. Through its binding to PtdIns(3,5)P$_2$, XopAP suppresses vacuolar acidification, hence preventing salicylic acid (SA)-induced stomatal closure, which is beneficial to *Xoc* infection in rice. In addition, stomatal closure induced by flg22 was also inhibited in transgenic plants overexpressing *XopAP*. We also show that XopAP impairs plant PAMP-triggered immunity (PTI) responses, such as reactive oxygen species (ROS) burst, callose deposition, and the expression of defense genes, thus enhancing the pathogenicity of *Xoc*.

RESULTS

XopAP contributes to *Xoc* virulence in rice

The annotation of XopAP as a lipase and a T3E protein of *Xoc* (Bogdanove et al., 2011) suggested a possible role in pathogen virulence. We therefore generated nine transgenic rice lines in the Nipponbare cultivar with constitutive expression of *XopAP* driven by the cauliflower mosaic virus (CaMV) 35S promoter via *Agrobacterium tumefaciens*-mediated transformation. We detected the accumulation of XopAP-HA (hyaluronic acid) in these transgenic lines by immunoblotting (Figure S1A). The independent homozygous *XopAP*-OX4 and *XopAP*-OX5 transgenic lines exhibited the highest protein abundance for XopAP of all lines and were selected for the following experiment. To test the contribution of XopAP to virulence, we deleted the *XopAP* gene in a wild-type strain BLS256 by nonmarker mutagenesis (Zou et al.,

2011), resulting in the mutant ΔXopAP. In addition, we generated the complemented strain CΔXopAP by providing the *XopAP* gene in *trans* (Table S1). We then individually inoculated the leaves of Nipponbare, a rice cultivar susceptible to BLS, with each of these three strains by needling (Zou et al., 2006) and by the spray method (Figure 1A, C). Indeed, the virulence (lesion length) of the mutant ΔXopAP was significantly lower ($P < 0.01$, t-test) than that caused by the wild-type strain at 14 d post-inoculation (dpi); importantly, the complemented strain CΔXopAP restored virulence to wild-type levels (Figure 1B). The XopAP-OX4 transgenic plants showed higher susceptibility (as measured by lesion lengths) to the three strains than the wild-type Nipponbare (Figure 1B). We noticed that the pathogen infection sites in Nipponbare are significantly smaller than those in XopAP-OX4 transgenic plants at 4 dpi, when bacterial suspensions at optical density of 600 nm (OD_{600}) = 0.5 were sprayed onto the leaf surface of
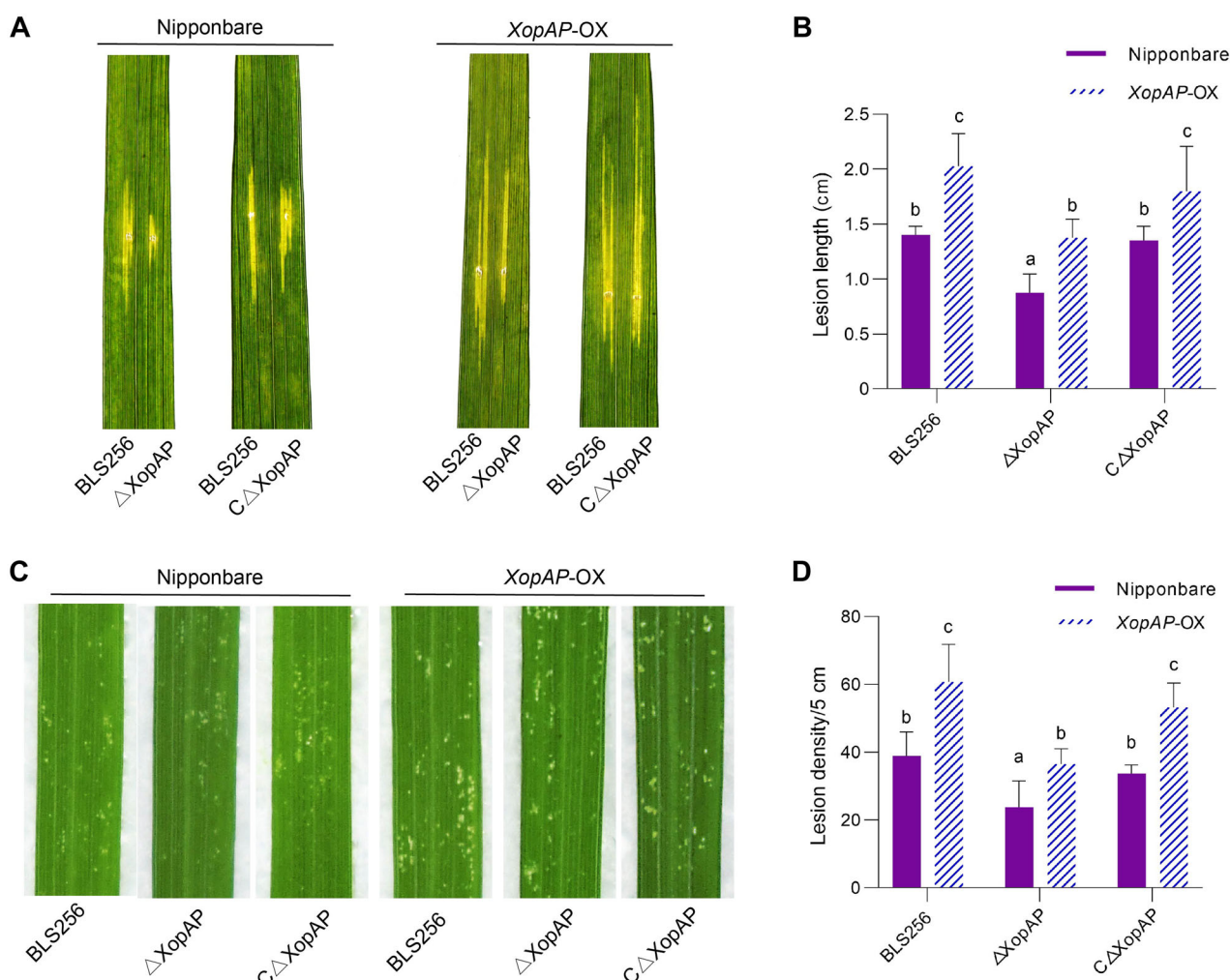

Figure 1. XopAP overexpression rice plants confer increased disease susceptibility

Four- to 6-week-old Nipponbare and transgenic rice plants overexpressing *XopAP* were inoculated with *Xoc* BLS256 (wild type, WT), the *XopAP* deletion mutant (ΔXopAP), and ΔXopAP complemented with *XopAP* (CΔXopAP). (**A**) Representative disease symptoms at 14 d post-inoculation (dpi) by leaf vein-piercing. (**B**) Quantification of disease lesion length at 14 dpi. (**C**) Representative disease symptoms at 3 dpi by spray inoculation. (**D**) Quantification of lesion density from 5-cm segments of infected leaves. These experiments were performed three times with similar results. Different lowercase letters indicate significant differences at $P < 0.05$, as determined by two-way analysis of variance with Tukey's test.

the tested rice plants (Figure 1D), implying that the presence of XopAP, either in the pathogen or in the host rice, enables rice stomata opening beneficially for bacterial invasions.

As in rice, transgenic *Arabidopsis* lines overexpressing *XopAP* were also significantly more susceptible to *Pst* DC3000. Since the COR-deficient mutant strain DB29 has lost the ability to enter plants through stomata (Brooks et al., 2004), we inoculated wild-type *Arabidopsis* Col-0 and the *XopAP*-OX lines *XopAP*-OX3 and *XopAP*-OX5 with *Pst* DC3000 and DB29, respectively, by spray inoculation to test whether the heterologous expression of *XopAP* might allow DB29 to successfully invade the host. Compared to the wild-type Col-0, both *XopAP*-OX3 and *XopAP*-OX5 transgenic lines were susceptible to DB29 inoculation, although less so than to *Pst* DC3000 (Figure S2A). In agreement with the disease symptoms, the growth of the *Pst* strains in the infected *XopAP*-OX3 and *XopAP*-OX5 lines was significantly higher than in Col-0 at 3 dpi (Figure S2B). We also spray-inoculated Col-0 and the *XopAP*-OX5 transgenic line with *P. syringae* pv. *maculicola* (*Psm*) ES4326, which is another virulent strain on *Arabidopsis*, and observed more severe disease symptoms with *XopAP*-OX5 than with Col-0 at 3 and 7 dpi (Figure S2C). The bacterial population in *XopAP*-OX3 and *XopAP*-OX5 lines was significantly higher than in

the wild type (Figure S2D). Collectively, these data suggest that XopAP may play a similar role as coronatine in interfering with plant stomatal closure during bacterial infection.

XopAP binds to PtdIns(3,5)P$_2$

A protein sequence alignment revealed that XopAP is conserved in *Xanthomonas citri*, but not in *X. oryzae* (Figure S3). We speculate that *Xoc* and *X. citri* both belong to the mesophyll pathogens that colonize their host locally at the infection site. We identified a highly conserved region in XopAP, from amino acids 74 to 201, that is predicted as a lipase domain by the online tool SMART (Figure S4A). These characteristics prompted us to investigate whether XopAP functions as a lipase via *in vitro* assays. Surprisingly, recombinant purified XopAP showed no lipase activity (Figure S4B), which raised the possibility that XopAP might bind to lipids instead. To test this hypothesis, we purified glutathione *S*-transferase (GST)-tagged XopAP and performed *in vitro* lipid-binding assays. Notably, we detected binding between recombinant XopAP and PtdIns(3,4)P$_2$, PtdIns(3,5)P$_2$, PtdIns(4,5) P$_2$, and PtdIns(3,4,5)P$_3$ (Figure 2B). In particular, XopAP displayed high affinity toward PtdIns(3,5)P$_2$ and PtdIns(3,4,5)P$_3$. As PtdIns(3,4,5)P$_3$ has not been detected in plants (Heilmann, 2016), we focused on PtdIns(3,5)P$_2$.
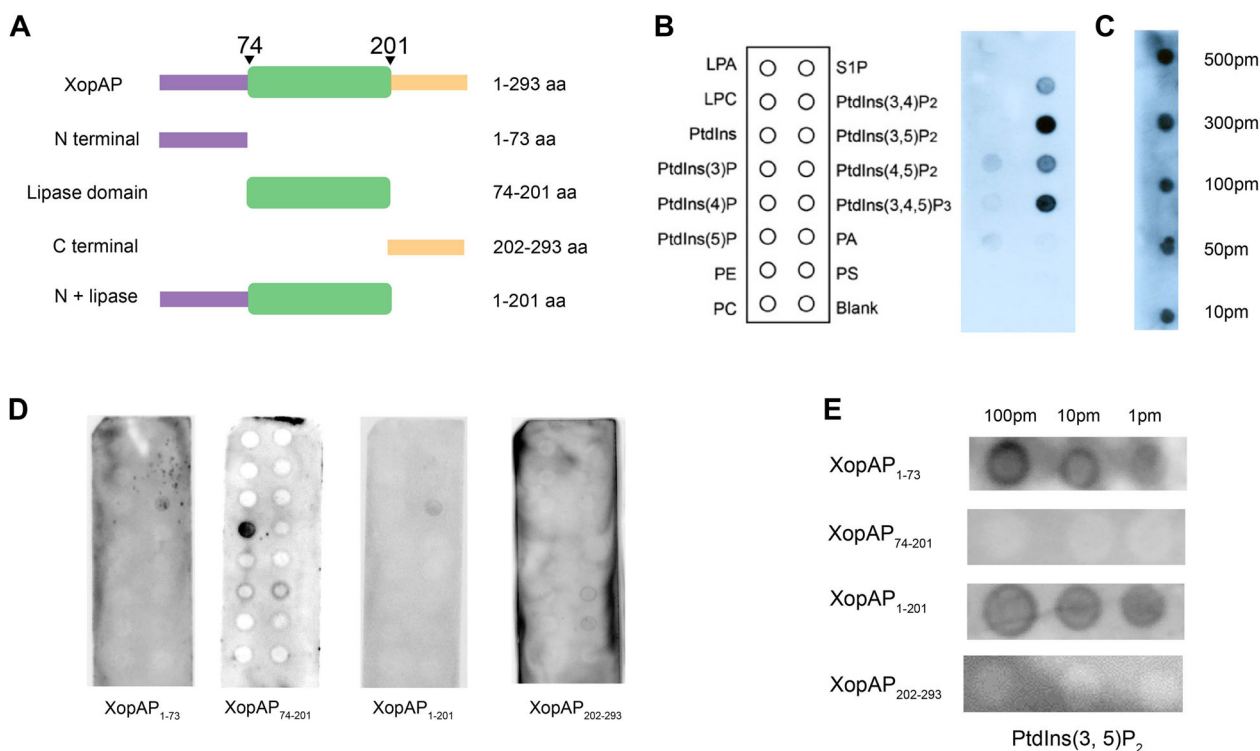

Figure 2. XopAP binds to PtdIns(3,5)P$_2$

(A) Schematic diagrams of full-length XopAP and four XopAP truncation variants, XopAP$_{1-73}$, XopAP$_{74-201}$, XopAP$_{1-201}$, and XopAP$_{202-293}$. Purple and orange lines indicate the N and C termini, respectively. The green box indicates the conserved lipase domain. Numbers indicate the amino acid residues. (B, D) Lipid-binding assays with recombinant XopAP and the four XopAP truncation variants. Five nanomolar of each recombinant protein (as glutathione (GST) fusions) was incubated with commercial PIP Strips. The lipid-binding proteins were detected by immunoblotting with an anti-GST antibody. (C, E) Estimation of the lipid-binding affinity of full-length XopAP and variants. Serial dilutions (500, 300, 100, 50, 10, and 1 pmol) of PtdIns(3,5)P$_2$ were spotted onto nitrocellulose membranes, which were then incubated with the GST-fusion proteins. The lipid-binding proteins were detected by immunoblotting with an anti-GST antibody.

To identify the functional domain responsible for binding to PtdIns(3,5)P$_2$, we generated four XopAP truncation variants (XopAP$_{1-73}$, XopAP$_{74-201}$, XopAP$_{1-202}$, and XopAP$_{202-293}$) (Figure S5A) and purified each recombinant protein in BL21(DE3) (Figure S5B). We determined that XopAP$_{1-73}$ and XopAP$_{1-202}$ retain binding capacity to PtdIns(3,5)P$_2$ (Figure 2D). Surprisingly, XopAP$_{74-201}$ bound strongly to PtdIns(3)P (Figure 2D), whereas full-length XopAP only exhibited weak binding with this lipid (Figure 2B). We speculate that this truncated variant undergoes a conformational change, resulting in an altered affinity toward PtdIns(3)P. We performed a Fat Blot assay to explore the interactions between XopAP variants and PtdIns(3,5)P$_2$. Accordingly, we spotted serial dilutions of PtdIns(3,5)P$_2$ onto a nitrocellulose membrane before incubating the membrane with each recombinant protein (full-length and truncated variants) and detected binding between PtdIns(3,5)P$_2$ and XopAP, XopAP$_{1-73}$ and XopAP$_{1-202}$ (Figure 2C, E).

A closer look at the predicted lipase domain of XopAP revealed the conservation of the Ser-131 residue in the characteristic lipase G-X-S-X-G motif (Figure S3). To assess the role of this conserved amino acid in PtdIns(3,5)P$_2$ binding, we generated the point mutant XopAP$_{S131A}$ by replacing Ser-131 with Ala. Importantly, we observed that recombinant XopAP$_{S131A}$ still binds to PtdIns(3,5)P$_2$ (Figure S5C). Together, these analyses demonstrate that the N terminus of XopAP is necessary for binding to PtdIns(3,5)P$_2$.

XopAP and V-PPase competitively bind to PtdIns(3,5)P$_2$

PtdIns(3,5)P$_2$ is located in the vacuolar membrane (McCartney et al., 2014; Heilmann, 2016). Since XopAP binds to PtdIns(3,5)P$_2$, we hypothesized that XopAP might also localize to the vacuole or vacuolar membrane. To test this hypothesis, we investigated the subcellular localization of XopAP in rice protoplasts using Arabidopsis KCO1 (K$^+$ channel, Ca^{2+}-activated, outward rectifying (1)) as a tonoplast marker (Czempinski et al., 2002; Voelker et al., 2006). We transfected rice protoplasts with constructs encoding AtKCO1-RFP (a fusion between AtKCO1 and red fluorescent protein (RFP)) or XopAP-GFP (a fusion between XopAP and green fluorescent protein (GFP)). We determined that the red fluorescence of AtKCO1-RFP largely overlaps with the green fluorescence of XopAP-GFP (Figure 3A). This result indicated that XopAP localizes to the tonoplast. The proton pump V-PPase is present on the tonoplast membrane (Maeshima and Yoshida, 1989; Kriegel et al., 2015). It has been reported that V-PPase can bind to PtdIns(3,5)P$_2$ and contributes to the acidification of vacuoles (Ferjani et al., 2011; Bak et al., 2013; Segami et al., 2018). We thus tested whether XopAP is involved in vacuolar acidification by conducting a competitive binding experiment. To this end, we incubated 5 nmol/L of each recombinant purified GST-tagged XopAP and V-PPase, individually or in combination, with membranes spotted with serial dilutions of lipids, followed by immunoblotting with anti-GST or anti-V-PPase antibody, respectively, to assess binding to PtdIns(3,5)P$_2$. We determined that the binding of V-PPase to PtdIns(3,5)P$_2$ decreases substantially when co-incubated with XopAP (Figure 3B). We conclude that XopAP and V-PPase compete to bind to PtdIns(3,5)P$_2$.

XopAP inhibits stomatal closure induced by SA

The greater susceptibility shown by XopAP-OX transgenic rice plants using two types of inoculation methods, especially spray inoculation, suggested that XopAP might interfere with
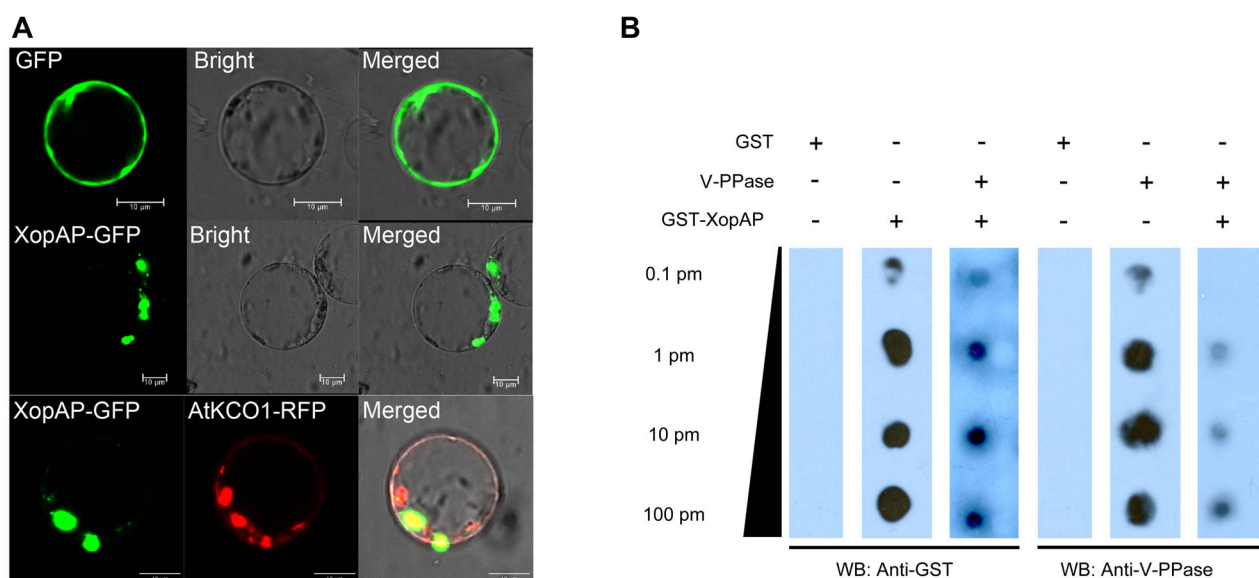

Figure 3. XopAP binds to PtdIns(3,5)P$_2$ in competition with vacuolar H$^+$-pyrophosphatase (V-PPase)
(A) Subcellular localization of XopAP in transiently transfected rice protoplasts. The coding sequences of *XopAP* and *AtKCO1* were cloned into the pRTVcGFP and pRTVcRFP vectors, respectively. The *XopAP-GFP* and *AtKCO1-RFP* constructs were co-transfected into rice protoplasts. AtKCO1 served as a tonoplast marker. Scale bars, 10 μm. (B) Assessment of lipid binding by XopAP and V-PPase. PtdIns(3,5)P$_2$ was serially diluted (100, 10, 1, and 0.1 pmol) and spotted onto nitrocellulose membranes, which were subsequently incubated with 5 nmol/L XopAP-GST (glutathione) or V-PPase. The binding of PtdIns(3,5)P$_2$ was determined by immunoblotting with anti-GST and anti-V-PPase antibodies.

stomatal immunity in plants. The plant defense hormone SA has been shown to induce stomatal closure in *Arabidopsis* (Zeng and He, 2010; Yekondi et al., 2018; Zamora et al., 2021), which prompted us to explore the role of XopAP in stomatal closure. Since endogenous SA and ABA play important roles in stomatal closure in plants, we determined their contents in Nipponbare and *XopAP*-OX transgenic plants. However, the concentrations of SA and ABA were not significantly different between Nipponbare and *XopAP*-OX transgenic lines (Figure S6). Consistent with previous studies, SA caused stomatal closure in Nipponbare, but we detected a weaker response to SA in *XopAP*-OX transgenic rice plants (Figure 4A). Indeed, we determined that SA treatment causes the closure of fewer stomata in both *XopAP*-OX4 and *XopAP*-OX5 transgenic lines compared to the wild type (Figure 4B).

Notably, the percentage of open stomata in both *XopAP*-OX4 and *XopAP*-OX5 transgenic lines was higher than that of the wild type, even in the absence of SA treatment (Figure 4B). To confirm this result, we carried out a water loss assay, during which we measured the fresh weight of detached leaves over time when maintained in dry air. We observed that *XopAP*-OX leaves lose water faster than the wild type (Figure S7). We obtained similar results in *Arabidopsis* lines overexpressing *XopAP* (Figure 4C), as evidenced by the diminished stomatal closure induced by SA treatment in these lines (Figure 4D).

XopAP suppresses SA-induced vacuolar acidification

Vacuolar acidification leads to stomatal closure. PtdIns (3,5)P$_2$ plays an important role in the regulation of vacuolar acidification in guard cells (Perez Koldenkova and
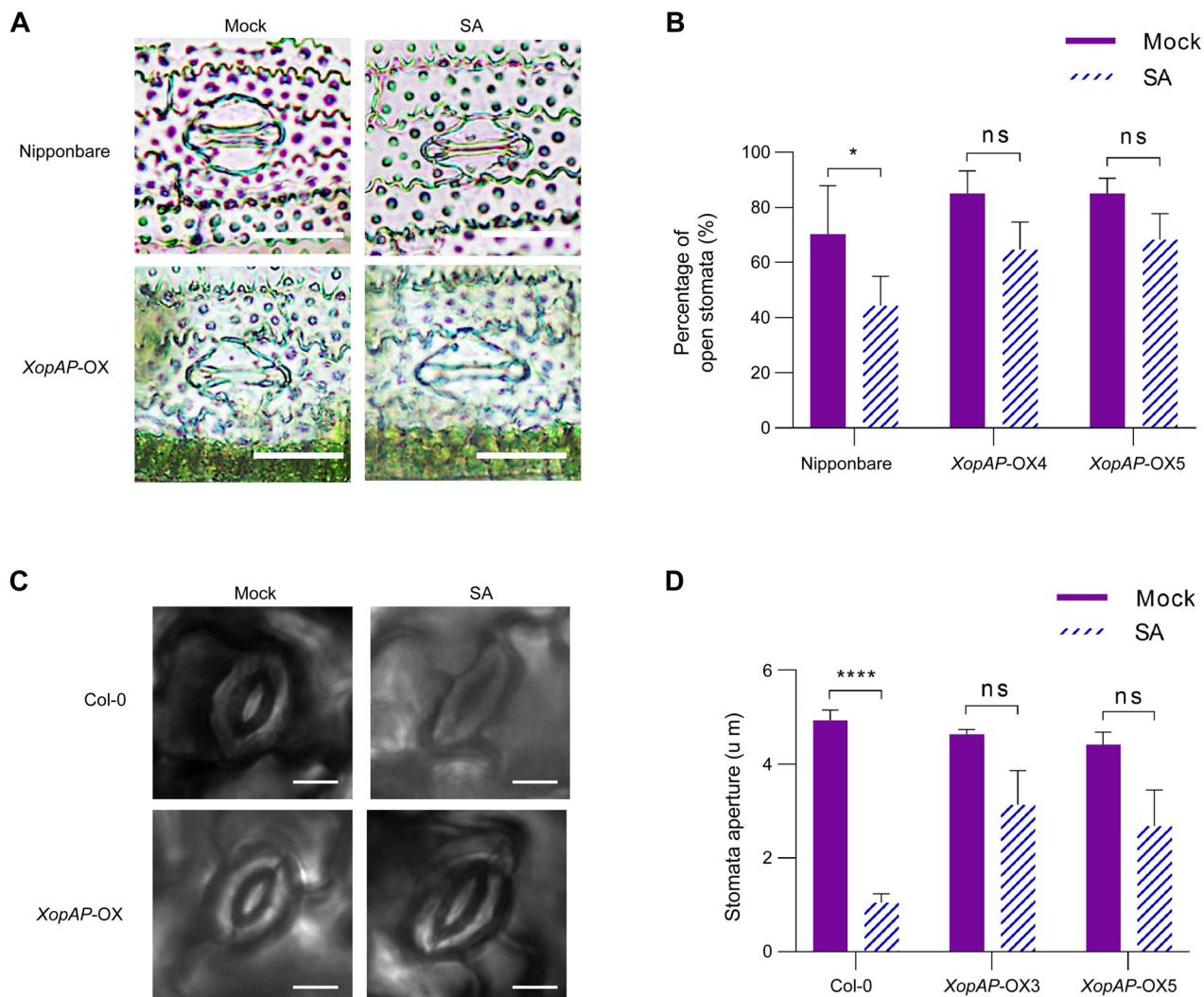

Figure 4. XopAP inhibits stomatal closure induced by salicylic acid (SA)
(**A**, **B**) Representative images (**A**) and percentage of open stomata (**B**) of rice epidermal stomata from Nipponbare and transgenic rice plants overexpressing *XopAP* under normal conditions or after treatment with 50 μmol/L SA. (**C**, **D**) Representative images of *Arabidopsis* stomata (**C**) and stomatal aperture (**D**) in epidermal peels from Col-0 or transgenic plants overexpressing *XopAP* under normal conditions or after treatment with 20 μmol/L SA. Scale bars, 10 μm. Values are shown as means ± SD of 100 stomata. Significant differences (ns, no significance; *$P = 0.037$; ****$P < 0.0001$) were determined by two-way analysis of variance with Tukey's test.

Hatsugai, 2017; Scholz-Starke, 2017). To determine the role of XopAP in stomatal closure, we followed the changes in vacuolar pH in *XopAP*-OX transgenic rice lines using the fluorescent dye acridine orange (AO) (Figure 5A). AO is protonated in acidic environments, resulting in emission intensity changes. We evaluated the extent of vacuolar acidification by calculating the fluorescence ratio between red fluorescence and green fluorescence (R/G) and represented the pH in confocal images according to a pseudo color scale (with blue indicating high pH and green indicating low pH). To specifically assess the contribution of PtdIns(3,5)P_2, which is synthesized by PtdIns3P 5-kinase (PI3P5K) (Morishita et al., 2002), we used a PIK-fyve inhibitor to block PI3P5K kinase activity and reduce PtdIns(3,5)P_2 production (Bak et al., 2013). We established that the vacuoles of Nipponbare become significantly acidified after SA treatment, as reflected by the over two-fold increase in the R/G ratio in these samples. Notably, we failed to detect a significant acidification of vacuoles in *XopAP*-OX transgenic lines, as the R/G ratio remained comparable regardless of SA treatment (Figure 5). The application of PIKfyve inhibitor blocked the acidification of

wild-type vacuoles by SA, while the same treatment induced the acidification of the vacuoles of *XopAP*-OX transgenic lines, with a 1.5-fold increase in the R/G ratio (Figure 5A, B). We performed the same assay using AO and LysoSensor in *Arabidopsis* lines. Consistent with the results obtained in rice, the vacuoles of the wild-type Col-0 became more acidified than those of *XopAP*-OX transgenic plants after SA treatment, whereas treatment with PIKfyve inhibitor reversed these results, with the *XopAP*-OX lines having a more acid vacuole than the wild type (Figure S8A). Indeed, the *XopAP*-OX transgenic plants showed a lower R/G ratio compared to Col-0 plants upon SA treatment, but their R/G ratio increased significantly in the presence of PIKfyve inhibitor and SA (Figure S8B). The fluorescence intensity of LysoSensor reflects the degree of acidification. We detected a weak fluorescence from the vacuoles of guard cells from completely open stomata (Figure S8C). After SA treatment, the stomata from the wild-type Col-0 closed and emitted a much stronger green fluorescence intensity from their vacuoles, while the *XopAP*-OX transgenic plants showed little change. Importantly, the green fluorescence detected in *XopAP*-OX
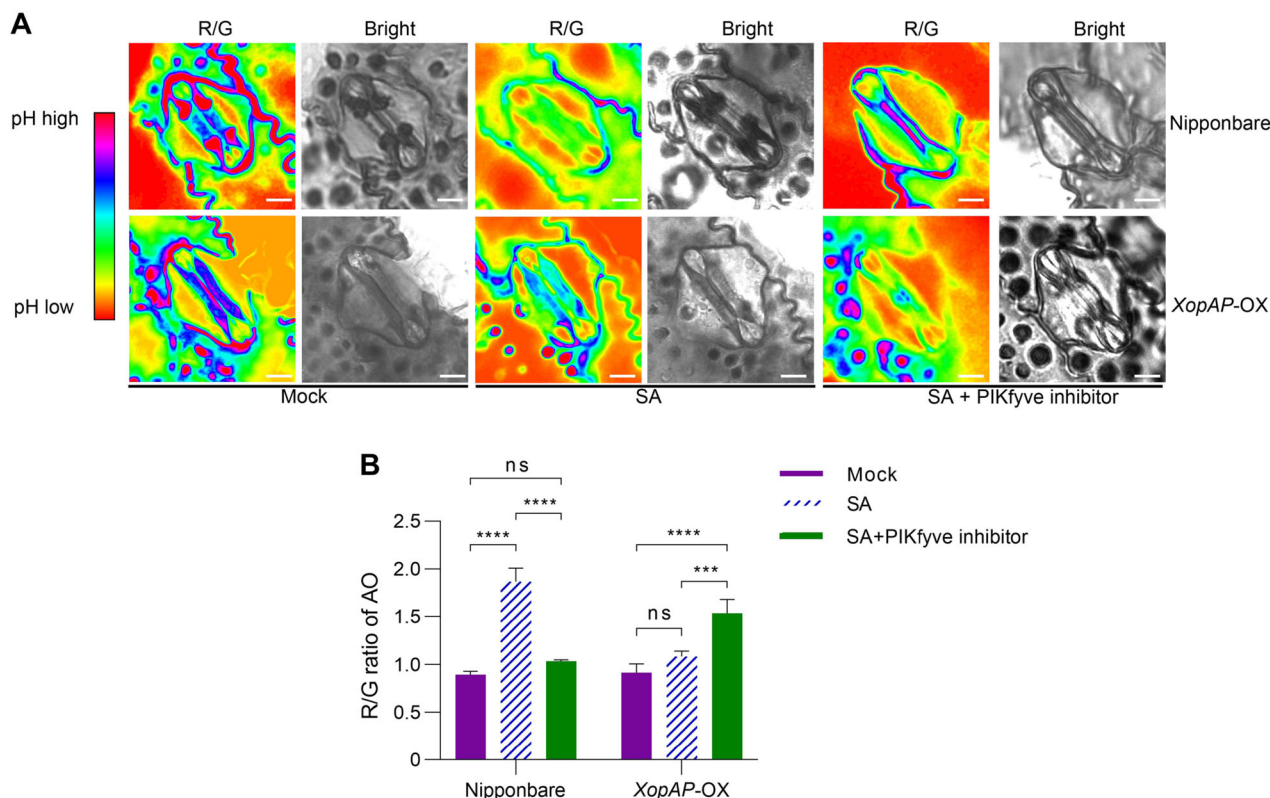

Figure 5. XopAP inhibits vacuolar acidification in rice resulting from salicylic acid (SA)-induced stomatal closure

(**A**) Representative images showing vacuolar acidification, as determined with acridine orange (AO) staining. Guard cells of Nipponbare and transgenic rice lines overexpressing XopAP (*XopAP*-OX) were stained for 2 h with 50 µmol/L AO before SA treatment, in the absence or presence of 10 µmol/L PIKfyve inhibitor, as indicated. Red/green (R/G) images represent the ratio between red fluorescence and green fluorescence and are displayed in pseudo color. Low R/G ratio (shown in blue) indicates high pH. High R/G ratio (shown in green) indicates low pH. Scale bars, 1 µm. (**B**) Quantification of vacuolar acidification, expressed as the mean values of R/G ratios. These experiments were performed three times with similar results. Significant differences (ns, no significance; ***$P = 0.0002$; ****$P < 0.0001$) were determined by two-way analysis of variance with Tukey's test.

transgenic plants increased markedly after the application of SA and PIKfyve inhibitor (Figure S6C). The mean fluorescence intensity in Col-0 rose nearly 10-fold after SA treatment, which was comparable to the increase in fluorescence observed in *XopAP*-OX transgenic plants after treatment with SA and PIKfyve inhibitor (Figure S8D). Therefore, the results obtained in rice and *Arabidopsis* suggest that XopAP blocks the acidification of the vacuolar lumen during SA-induced stomatal closure.

The expression of *XopAP* in transgenic plants inhibits PTI and bacterial resistance

Reactive oxygen species accompany PTI reaction (Yuan et al., 2021) and induce stomatal closure to limit pathogen invasion (Kadota et al., 2014; Li et al., 2014). As ROS production is an important part of stomatal immunity, we asked whether XopAP affects the ROS burst elicited by flg22. Accordingly, we estimated ROS levels and accumulation pattern in *XopAP*-OX transgenic plants via 3,3′-diaminobenzidine (DAB) staining and luminol-based chemiluminescence assays. As shown in Figure 6A, compared to wild-type Col-0, both *XopAP*-OX3 and *XopAP*-OX5 transgenic lines showed a lighter brown color after flg22 treatment, indicating lower levels of ROS revealed by DAB staining. We obtained similar results when quantifying the ROS burst of Nipponbare and *XopAP*-OX transgenic rice lines in response to flg22 treatment by the luminol-horseradish peroxidase chemiluminescence assay.

The higher ROS levels measured in Nipponbare indicated that XopAP prevents the flg22-induced ROS burst (Figure 6B). The more severe disease symptoms seen in *XopAP*-OX transgenic plants (Figures 1, S2) suggested that XopAP may interfere with plant immune responses, which we quantified by scoring the extent of callose deposition and the expression levels of defense-related genes in Col-0 and transgenic *Arabidopsis* lines. We determined that callose deposition levels in the wild-type Col-0 are significantly higher relative to both *XopAP*-OX3 and *XopAP*-OX5 transgenic lines in response to flg22 (Figure 6C, D). We then used reverse transcription quantitative polymerase chain reaction (RT-qPCR) to estimate the relative expression levels of early defense response genes (*FRK1* (*flg22-INDUCED RECEPTOR-LIKE KINASE1*); At2g17740, encoding a cysteine/histidine-rich C1 domain family protein; *GSL5* (*GLUCAN SYNTHASE-LIKE5*), and *FLS2* (*FLAGELLIN-SENSITIVE2*)) induced by flg22. Relative *FRK1* and At2g17740 transcript levels were much lower in both *XopAP*-OX3 and *XopAP*-OX5 transgenic lines than in Col-0 3 h after flg22 induction (Figure 6E). Similarly, the *GSL5* expression was lower in the *XopAP*-OX lines compared to Col-0 after 6 h. We detected no significant differences in *FLS2* expression levels between Col-0 and the transgenic lines. Collectively, these data indicate that XopAP inhibits PTI responses in plants, thereby enhancing the virulence of *Xoc* pathogens.

XopAP inhibits stomatal closure induced by flg22

Previous studies have shown that flg22 can induce stomatal closure in plants (Melotto et al., 2006; Zhang et al., 2008; Guzel Deger et al., 2015; Bharath et al., 2021; Zou et al., 2021). Considering that XopAP inhibits the PTI response in plants, we suspected that XopAP might also be involved in flg22-mediated stomatal closure. Consistent with our hypothesis, flg22 stimulated stomatal closure in Nipponbare, but not in *XopAP*-OX transgenic rice plants (Figure S9A). Indeed, the percentage of open stomata in both *XopAP*-OX4 and *XopAP*-OX5 transgenic lines treated with flg22 was significantly higher than in the wild-type Nipponbare (Figure S9B). We obtained similar results in *XopAP*-OX transgenic *Arabidopsis* relative to the wild-type Col-0 (Figure S9C), as evidenced by the suppression of stomatal closure in the *XopAP*-OX lines when treated with flg22 (Figure S9D).

DISCUSSION

Stomatal immunity is an important basic disease prevention system of plants. In order for plant pathogenic bacteria to enter plant cells, they must first overcome this stomatal immunity. The T3E HopM1 of *Pst* DC3000 was shown to inhibit the two early PTI responses, ROS burst and stomatal immunity, relying on 14-3-3 proteins (Lozano-Duran et al., 2014). Few studies have explored the mechanism by which pathogenic effector proteins interfere with stomatal immunity in rice. In this study, we discovered an effect for XopAP on stomatal closure in plants. XopAP contributes to *Xoc* virulence in rice plants by inhibiting plant stomatal immunity. XopAP binds to lipids and inhibits vacuolar acidification caused by the translocation of protons into vacuoles upon SA induction. Following vacuolar acidification, the vacuole changes its shape and decreases its turgor pressure, which leads to stomatal closure. With the help of XopAP, the pathogen can invade plant cells more quickly (Figure 7). Recently, XopC2 from *Xoc* RS105 was reported to activate jasmonic acid (JA) signaling by degrading the JAZ transcriptional repressors, forcing stomatal opening (Wang et al., 2021). Although the function of XopC2 in the BLS256 strain has not been established, we believe that XopC2 and XopAP inhibit stomatal immunity to different extents. This difference may also explain why *Xoc* still retains the ability to invade rice through stomata in the absence of XopC2 or XopAP alone. In addition, XopC2 enhances JA signaling, while XopAP may interfere with SA signaling in plants, indicating that XopAP and XopC2 act on independent cellular activities in plants.

Bioinformatics analysis showed that XopAP has a typical lipase domain, raising the possibility that XopAP might interfere with plant immune responses by degrading lipids to produce secondary metabolites. However, we detected no *in vitro* lipase activity when we tested recombinant XopAP. Lipases are present in almost all organisms, where they play key roles in the digestion, transport, and shearing of lipids (such as triglycerides, fats, and oils) (Svendsen, 2000). Most lipases act at specific positions on the glycerol skeleton of a lipid. Glycerophospholipids are the main components of biological membranes and participate in many signaling

pathways (Van Meer et al., 2008). Previous research has revealed that lipid signaling is a fundamental participant in cell signaling (Dinasarapu et al., 2011). Lipid signaling can be initiated by either G protein-coupled receptors or nuclear receptors, and many different types of lipids have been found to act as signaling molecules or as part of a second messenger system (Eyster, 2007). Lipases are involved in various biological processes, from lipid metabolism to cell signaling and inflammation (Spiegel et al., 1996). Additionally, due to

their industrial prospects and their use in biotechnology and organic chemistry, microbial lipases have become the preferred source of lipid production and processing (Hasan et al., 2006). Therefore, there is an increasing interest in bacterial lipases.

Understanding the molecular mechanisms by which plant pathogens cause diseases is a first step toward effective disease control (Fu and Dong, 2013). Effector proteins often interfere with the physiological and biochemical functions of
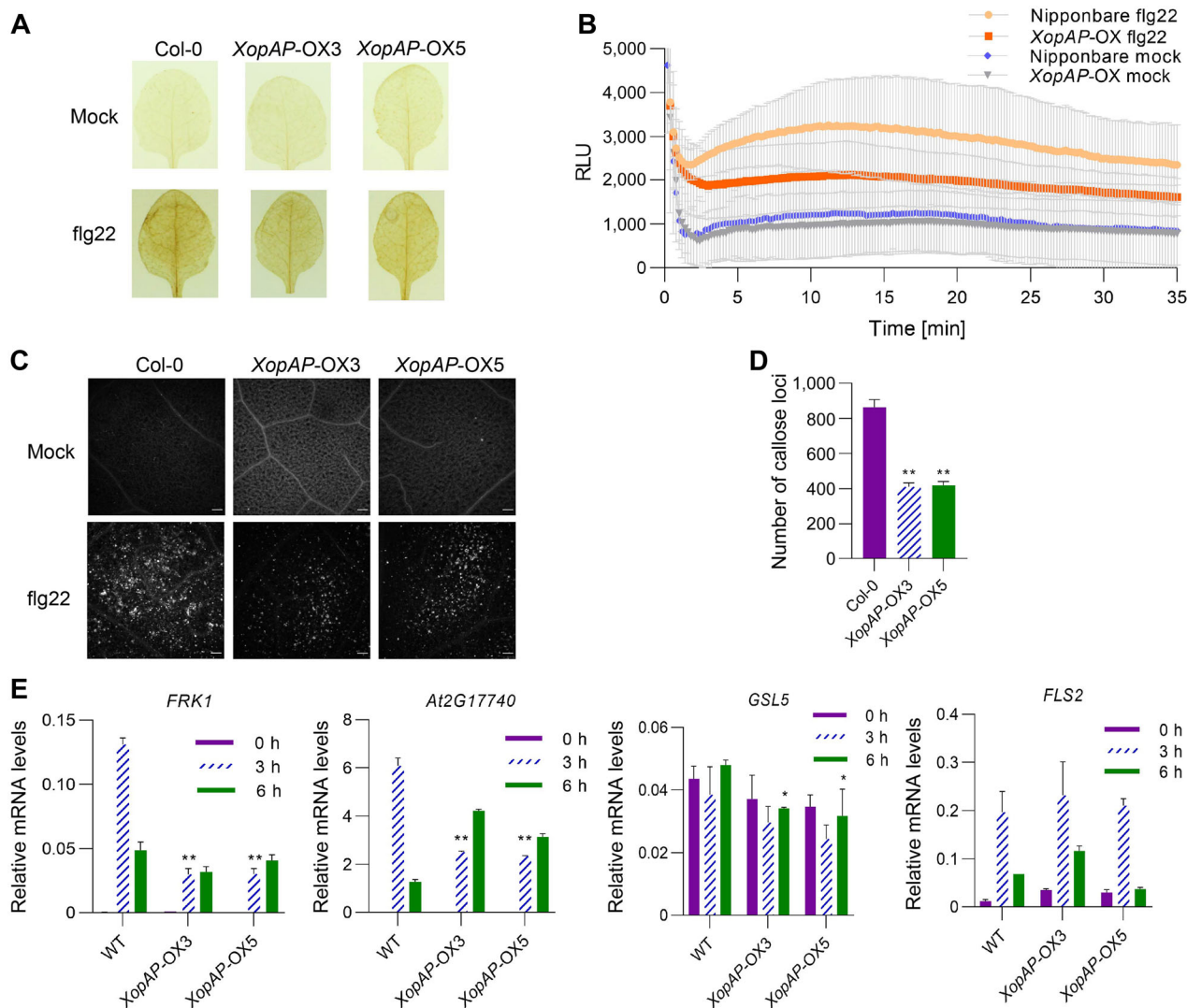

Figure 6. The overexpression of *XopAP* in transgenic plants inhibits pathogen-associated molecular pattern-triggered immunity (PTI) and bacterial resistance

(A) Detection of H_2O_2 levels by 3,3′-diaminobenzidine (DAB) staining in 4-week-old Col-0 and transgenic lines overexpressing *XopAP* 1 h after injection with 1 μmol/L flg22. Leaves of six independent plants were tested per line. (B) Time course of reactive oxygen species (ROS) production. The ROS burst was measured in 4-week-old Nipponbare and transgenic rice lines overexpressing *XopAP* using a luminol-horseradish peroxidase chemiluminescence assay (Leslie and Heese, 2014). Leaf discs were first soaked in water for 10 h and then transferred to a solution containing 34 mg/L luminol, 20 mg/L horseradish peroxidase, and 100 nmol/L flg22. The luminescence was recorded as relative light units with a GloMax 20/20 single tube luminometer (Promega). (C) Callose deposition in the leaves of 4-week-old Col-0 and transgenic lines overexpressing *XopAP*. Leaves were injected with 1 μmol/L flg22 and stained for callose as described in Methods. (D) Quantification of callose deposits, based on the number of fluorescent foci. Significant differences (*$P < 0.05$; **$P < 0.01$) were determined by one-way analysis of variance (ANOVA) with Tukey's test. (E) Relative expression levels of *FRK1*, At2g17740, *GSL5*, and *FLS2* in 4-week-old Col-0 and transgenic lines overexpressing *XopAP*, as measured by reverse transcription quantitative polymerase chain reaction. Leaves were infiltrated with 1 μmol/L flg22 for 3 or 6 h before samples were collected. *eEF-1α* was used as an internal reference gene. These experiments were performed three times with similar results. Significant differences (*$P < 0.05$; **$P < 0.01$) were determined by two-way ANOVA with Tukey's test.
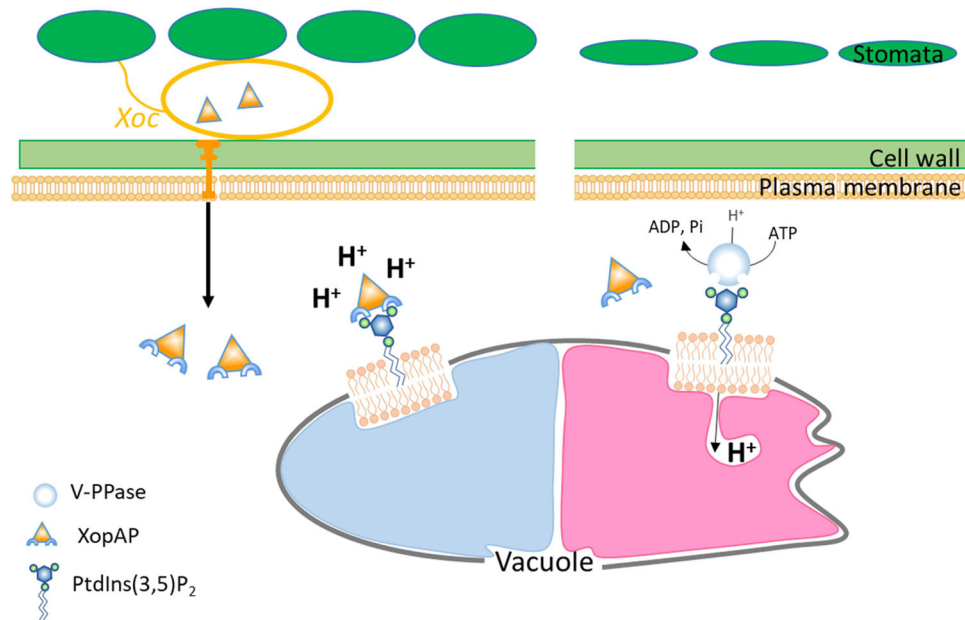
Figure 7. Proposed model for the function of XopAP
XopAP, a T3E protein from the rice pathogen *Xoc*, binds to the signaling lipid PtdIns(3,5)P$_2$ that is widely distributed in plant cells. PtdIns(3,5)P$_2$ localizes to the tonoplast membrane and plays an important role in the regulation of vacuolar pH. During salicylic acid (SA)-induced stomatal closure, XopAP inhibits vacuolar acidification by binding to PtdIns(3,5)P$_2$, which prevents protons from being pumped into the vacuole. XopAP thus forces stomata to remain open, which is conducive to pathogen infection.

plants by targeting host proteins and DNA. However, XopAP appears to bind specifically to a derivative of phosphatidylinositol. Lipids, especially phospholipids, which are important components of various membrane structures, play an indispensable role in plant signal transduction. As with most effector proteins, the N terminus of the amino acid sequence is the secretion and transport signal region, while the C terminus carries the functional domain. The N terminus of XopAP was essential for binding to PtdIns(3,5)P$_2$, whereas its lipase-like domain bound to PtdIns(3)P. Furthermore, a point mutation in a conserved amino acid did not affect XopAP binding to PtdIns(3,5)P$_2$. Bioinformatics analysis of XopAP failed to detect known lipid-binding domains. Coupled with the lack of a 3D structure, the key amino acid responsible for binding lipids remains to be identified.

PtdIns(3,5)P$_2$ is required for the regulation of distinct ion channels on endosomes and lysosomes, as well as the acidification of vacuoles (Hasegawa et al., 2017). In mutants lacking V-PPase or V-ATPase activity, vacuolar acidification is inhibited due to the absence of H$^+$ pumps (Bak et al., 2013). Furthermore, inward currents regulated by chloride channel a (CLC-a), an anion/H$^+$ exchanger, are suppressed by PtdIns(3,5)P$_2$, leading to vacuolar acidification (Carpaneto et al., 2017). The above reports suggest that the binding of XopAP to PtdIns(3,5)P$_2$ may cause stomatal reopening by the same mechanism whether induced by ABA or SA. The rice genome harbors 10 genes encoding PtdIns3P 5-kinases (PI3P5Ks). Since XopAP binds to PtdIns(3,5)P$_2$, its binding may affect PtdIns(3,5)P$_2$ levels in plants. Therefore, future

studies should test PtdIns(3,5)P$_2$ contents in rice plants inoculated with the BLS256 or *XopAP* mutant strains. Additionally, the effect on lipid composition in *XopAP* transgenic plants should be determined.

Our study also showed that XopAP inhibits the ROS burst, which normally promotes stomatal closure in plants. The receptor-like cytoplasmic kinase BIK1, a component of the FLS2 immune receptor complex, not only positively regulates flg22-triggered calcium influx but also directly phosphorylates the NADPH oxidase RESPIRATORY BURST OXIDASE HOMOLOG D (RbohD) at specific sites in a calcium-independent manner to enhance ROS production (Kadota et al., 2014; Li et al., 2014). Whether XopAP also participates in this signaling pathway is unclear. Notably, XopAP inhibited the callose deposition caused by flg22, indicating that XopAP contributes to flg22 perception or signal transduction.

Our results suggest that the *Xoc* T3E protein XopAP functions as a repressor of stomatal closure by interfering with vacuolar acidification. The defense responses mounted by plants upon *Xoc* infection are conserved in rice and *Arabidopsis*, which is counteracted by XopAP via suppression of stomatal immunity, an early defense event in plants.

MATERIALS AND METHODS

Plant materials and bacterial strains
Oryza sativa ssp. *japonica* cv. Nipponbare and *Arabidopsis thaliana* accession Columbia-0 (Col-0) were used as the wild

types and to generate transgenic plants. *Arabidopsis* plants were grown at 22 °C with 50% relative humidity under a 12-h-light/12-h-dark photoperiod. *A. tumefaciens* and *Escherichia coli* strains were cultivated in Luria-Bertani medium at 28 °C and 37 °C, respectively. *Xanthomonas oryzae* pv. *oryzicola* was cultured in nutrient agar medium at 28 °C. The following antibiotics concentrations were used: 25 µg/mL rifampicin, 100 µg/mL ampicillin, and 50 µg/mL kanamycin.

Generation of transgenic plants

For transgenic rice plants, the *XopAP* coding sequence with an in-frame *HA* tag sequence at its 3′ end was cloned into the pCAMBIA 1300 vector to place *XopAP-HA* expression under the control of the cauliflower mosaic virus (CaMV) 35S promoter. After confirmation by sequencing, the resulting *35S: XopAP-HA* construct was transformed into *Agrobacterium* strain EHA105. Transgenic rice plants were obtained by infecting rice callus with *Agrobacterium* cultures by Boyuan (Wuhan, China). The accumulation of XopAP was confirmed by immunoblotting.

For transgenic *Arabidopsis* plants, the coding sequence of *XopAP* was amplified with the primers XopAP_F/_R (Table S2) and cloned into pMDC83-*35S:GFP* with an LR clonase II enzyme mix kit (Invitrogen). *Arabidopsis* Col-0 was transformed with *Agrobacterium* strain GV3101 harboring the *35S: XopAP-GFP* construct using the floral dipping method (Logemann et al., 2006). Primary transgenic seedlings were selected on half-strength Murashige and Skoog medium containing 10 µg/L hygromycin. The accumulation of XopAP was confirmed by immunoblotting.

Construction of the *XopAP* deletion mutant and complemented strains

To generate the *XopAP* deletion mutant (Δ*XopAP*), genomic fragments upstream and downstream of *XopAP* were amplified with the primers XopAP_LF/_LR and XopAP_RF/_RR (Table S2) and cloned into the plasmid pKMS1. The resulting plasmid pKMS1-XopAP was introduced into *Xoc* BLS256 via electroporation. After homologous recombination, positive colonies were screened as described by Zou et al. (2011).

To generate the *XopAP* complemented strain (CΔ*XopAP*), a PCR product encoding XopAP-FLAG was generated with the primers XopAP_F/_R (Table S2) and then cloned into the vector pHM1 at the *EcoR* I/*Sal* I restriction sites. After confirmation by sequencing, the plasmid pHM1-XopAP was transformed into the Δ*XopAP* mutant via electroporation. Positive colonies were selected for antibiotic selection and confirmed by PCR amplification. The primers and plasmids used are listed in Tables S1 and S2.

Virulence assays

Plants were inoculated by syringe infiltration, leaf vein-piercing, and spray inoculation to assess the virulence of bacterial strains. For inoculation by hand infiltration, bacteria were resuspended at a cell density of 1×10^6 colony forming units (CFU)/mL in 10 mmol/L MgCl$_2$. The inoculum was injected into rice or *Arabidopsis* leaves with needleless syringes. The bacterial population in plant leaves was monitored 3 and 5 dpi. For leaf vein-piercing inoculation, 6-week-old rice leaves were inoculated with a cell suspension at 1×10^9 CFU/mL in cell density of the indicated *Xoc* strains by punching two small holes on either side of the vein with a pair of needles. Lesion lengths were measured at 2 weeks after inoculation (Cai et al., 2014). For spray inoculation, 4-week-old rice or *Arabidopsis* plants were sprayed with a bacterial suspension at a cell density of 5×10^8 CFU/mL resuspended in 10 mmol/L MgCl$_2$ containing 0.05% (v/v) Silwet L-77. The number of lesions observed for each *Xoc* strain was counted from a 5-cm segment of infected rice leaves at 5 dpi. The growth of *Pseudomonas syringae* in *Arabidopsis* leaves was evaluated as reported previously (Chen et al., 2017).

Protein production in *E. coli* and purification

The coding sequences for full-length *XopAP* and truncated *XopAP* fragments were cloned into pGEX-5X-1. The production and purification of the recombinant proteins were based on previously published methods, with modifications (Harper and Speicher, 2011). Briefly, *E. coli* BL21(DE3) cells harboring each vector were induced to produce the recombinant protein by the addition of isopropyl-thio-β-D-galactoside (IPTG, final concentration of 0.1 mmol/L) when the culture reached OD$_{600}$ of 0.4 in LB medium. Cells were collected by centrifuge at 13 000 rpm for 20 min at 4 °C and resuspended in 30 mL binding buffer ($1\times$ phosphate buffered saline (PBS) pH 7.0, 1 mmol/L phenylmethylsulfonyl fluoride, 5 mmol/L dithiothreitol, and $1\times$ protease inhibitor cocktail) after a 12-h induction at 24 °C. The supernatant was incubated with glutathione Sepharose 4B resin (GE Healthcare) for 2 h after sonication. The GST-tagged proteins bound to the resin were washed with five column volumes of $1\times$ PBS and then eluted in elution buffer (50 mmol/L Tris-HCl, pH 8.0, 100 mmol/L NaCl, and 10 mmol/L reduced glutathione).

RT-qPCR analysis

Four-week-old Col-0 and *XopAP* transgenic *Arabidopsis* plants were treated with 1 µmol/L flg22 for 3 or 6 h. Total RNA was extracted using RNAiso Plus reagent (Takara, Dalian, China). First-strand complementary DNA (cDNA) was synthesized with TransScript® One-Step gDNA Removal and cDNA Synthesis SuperMix (TransGen, Beijing, China). Gene expression levels were determined by qPCR using an Applied Biosystems 7500 Real-Time PCR System (ThermoFisher, USA). The internal control gene *eEF-1α* was used for normalization. The relative expression levels of three technical replicates were evaluated using the $2^{-\Delta\Delta C_t}$ method.

Lipid-binding assay

Lipid-binding assays were conducted as described previously (Dowler et al., 2002; Han et al., 2020). PIP Strips (Echelon, USA) were blocked in blocking buffer ($1\times$ PBS, 0.1% (v/v) Tween 20, and 3% (w/v) bovine serum albumin) for 1 h. The strips were incubated in fresh blocking buffer for 1 h

containing 5 nmol/L of recombinant purified XopAP or XopAP truncated variants. After washing three times for 15 min each, the membranes were incubated for 1 h with anti-GST antibody in fresh blocking buffer. After three washes for 15 min each, the membranes were incubated for 1 h with horseradish peroxidase (HRP)-conjugated mouse secondary antibody in fresh blocking buffer. The lipid-binding protein was detected by Pierce™ ECL Western Blotting Substrate (Thermo Scientific).

Stomatal aperture assay

Stomatal observations and quantifications were conducted as described previously (Bak et al., 2013; Zhang et al., 2021). Four-week-old *Arabidopsis* leaves or epidermal fragments of rice were incubated in stomata recovery buffer (30 mmol/L KCl, 10 mmol/L MES-KOH, and 10 mmol/L $CaCl_2$, pH 6.05) for 3 h under bright light to fully open stomata. *Arabidopsis* leaves and epidermal fragments were then treated with 20 μmol/L SA or 10 μmol/L flg22. Stomata were observed and photographed using a confocal laser scanning microscope (Carl ZEISS LSM 700). At least 100 stomata were randomly captured for each treatment. Aperture size and the percentage of open stomata were measured in ImageJ software.

Water loss assays

Leaves of 4-week-old Nipponbare and *XopAP* transgenic rice at the same leaf position were selected, and their initial wet weight was measured. Water loss in dry air was measured every 10 min for the first hour and every 30 min thereafter.

Vacuolar lumenal acidification measurements

The acidification of guard cell vacuoles was detected with two fluorescent dyes, AO (Invitrogen) and LysoSensor (LysoSensor Green DND-189, Invitrogen), following a method described previously (Bak et al., 2013). Plant epidermal fragments were stained for 2 h with 50 μmol/L AO or for 30 min with 4 μmol/L LysoSensor. Epidermal fragments were then treated with 20 μmol/L SA in the absence or presence of 10 μmol/L PIKfyve inhibitor and observed by confocal laser scanning microscopy (Carl ZEISS LSM 700). The excitation/emission wavelengths for AO were 488 nm/615 to 660 nm (red channel) and 530 to 540 nm (green channel). The excitation/emission wavelengths of LysoSensor were 458 nm/505 to 530 nm. The fluorescence intensity was calculated in ImageJ software to evaluate the acidification level of vacuoles.

Callose deposition assay

Callose deposition assays were conducted as described previously (Daudi et al., 2012), with minor modifications. Briefly, 4-week-old *Arabidopsis* plants were infiltrated with 1 μmol/L flg22 and exposed to high humidity for 12 h. Rosette leaves were placed in 95% (v/v) ethanol to remove chlorophylls for 20 h. Leaves were then incubated with 0.05% (w/v) methyl blue in 100 mmol/L K_2HPO_4 (pH 9.0) for 4 h in darkness. Callose deposition was observed with a confocal laser scanning microscope (Carl ZEISS LSM 700).

The number of callose deposits was counted with ImageJ software.

Reactive oxygen species assay

The *in situ* detection of H_2O_2 was conducted using an adaptation of the 3,3′-diaminobenzidine (DAB) staining method (Daudi and O'Brien, 2012). Briefly, 4-week-old *Arabidopsis* plants were pretreated with 1 μmol/L flg22 for 1 h. Leaves were then stained in 0.1% (w/v) DAB solution in 10 mmol/L Na_2HPO_4 and 0.05% (v/v) Tween 20, pH 3.0, for 6 h in darkness and subsequently boiled in bleaching solution (ethanol : acetic acid : glycerol, 3:1:1 v/v/v) for 20 min. The leaves were then soaked in 95% (v/v) ethanol until chlorophylls were completely removed. Photographs were taken on a plain white background with uniform lighting.

Salicylic acid and ABA measurements

Salicylic acid and ABA levels were determined using plant SA/ABA enzyme-linked immunosorbent assay kits according to the manufacturer's instructions (Zhen Ke Biological Technology Co., Ltd, Shanghai). Briefly, 200 mg of 4-week-old rice leaves was ground into powder in liquid nitrogen. One milliliter of extraction buffer (90% (v/v) methanol and 0.1% (v/v) formic acid) was added to the powder to extract SA/ABA. Fifty microliters of diluted sample and 100 μL of HRP-conjugated reagent were incubated at 37 °C for 1 h. To each sample, 50 μL of substrate and 50 μL of stop solution were sequentially added to each well before measuring the optical density at 450 nm.

CONFLICTS OF INTEREST

The authors declare they have no conflicts of interest associated with this work.

AUTHOR CONTRIBUTIONS

Z.Q.F., G.Y.C., and L.Y.L. designed experiments. L.Y.L. performed most of the experiments and analyzed data. Y.L., Z.Y. X., and L.F.Z provided some constructs used in this study. H. C. and J.Y.Z. supervised the experiments and analyzed data. L.Y.L. wrote the paper. B.M., F.Q.L., Z.Q.F., and G.Y.C. revised the manuscript. All authors read and approved of the final manuscript.

Edited by: Suomeng Dong, Nanjing Agricultural University, China

REFERENCES

Bak, G., Lee, E.J., Lee, Y., Kato, M., Segami, S., Sze, H., Maeshima, M., Hwang, J.U., and Lee, Y. (2013). Rapid structural changes and acidification of guard cell vacuoles during stomatal closure require phosphatidylinositol 3,5-bisphosphate. Plant Cell 25: 2202–2216.

Bharath, P., Gahir, S., and Raghavendra, A.S. (2021). Abscisic acid-induced stomatal closure: An important component of plant defense against abiotic and biotic stress. Front. Plant Sci. 12: 615114.

Blümke, A., Falter, C., Herrfurth, C., Sode, B., Bode, R., Schäfer, W., Feussner, I., and Voigt, C.A. (2014). Secreted fungal effector lipase releases free fatty acids to inhibit innate immunity-related callose formation during wheat head infection. Plant Physiol. 165: 346–358.

Bogdanove, A.J., Koebnik, R., Lu, H., Furutani, A., Angiuoli, S.V., Patil, P.B., Van Sluys, M.A., Ryan, R.P., Meyer, D.F., Han, S.W., Aparna, G., Rajaram, M., Delcher, A.L., Phillippy, A.M., Puiu, D., Schatz, M. C., Shumway, M., Sommer, D.D., Trapnell, C., Benahmed, F., Dimitrov, G., Madupu, R., Radune, D., Sullivan, S., Jha, G., Ishihara, H., Lee, S.W., Pandey, A., Sharma, V., Sriariyanun, M., Szurek, B., Vera-Cruz, C.M., Dorman, K.S., Ronald, P.C., Verdier, V., Dow, J.M., Sonti, R.V., Tsuge, S., Brendel, V.P., Rabinowicz, P.D., Leach, J.E., White, F.F., and Salzberg, S.L. (2011). Two new complete genome sequences offer insight into host and tissue specificity of plant pathogenic Xanthomonas spp. J. Bacteriol. 193:: 5450–5464.

Brooks, D.M., Hernández-Guzmán, G., Kloek, A.P., Alarcón-Chaidez, F., Sreedharan, A., Rangaswamy, V., Peñaloza-Vázquez, A., Bender, C. L., and Kunkel, B.N. (2004). Identification and characterization of a well-defined series of coronatine biosynthetic mutants of Pseudomonas syringae pv. tomato DC3000. Mol. Plant Microbe Interact. 17: 162–174.

Büttner, D. (2016). Behind the lines–actions of bacterial type III effector proteins in plant cells. FEMS Microbiol. Rev. 40: 894–937.

Cai, L., Zou, L., Ling, G., Xue, X., Zou, H., and Chen, G. (2014). An inner membrane protein (Imp) of Xanthomonas oryzae pv. oryzicola functions in carbon acquisition, EPS production, bacterial motility and virulence in rice. J. Integr. Agric. 13: 2656–2668.

Carpaneto, A., Boccaccio, A., Lagostena, L., Di Zanni, E., and Scholz-Starke, J. (2017). The signaling lipid phosphatidylinositol-3,5-bisphosphate targets plant CLC-a anion/H($^+$) exchange activity. EMBO Rep. 18: 1100–1107.

Chen, H., Chen, J., Li, M., Chang, M., Xu, K., Shang, Z., Zhao, Y., Palmer, I., Zhang, Y., McGill, J., Alfano, J.R., Nishimura, M.T., Liu, F., and Fu, Z.Q. (2017). A bacterial type III effector targets the master regulator of salicylic acid signaling, NPR1, to subvert plant immunity. Cell Host Microbe 22: 777–788.

Czempinski, K., Frachisse, J.M., Maurel, C., Barbier-Brygoo, H., and Mueller-Roeber, B. (2002). Vacuolar membrane localization of the Arabidopsis 'two-pore' K$^+$ channel KCO1. Plant J. 29: 809–820.

Daudi, A., Cheng, Z., O'Brien, J.A., Mammarella, N., Khan, S., Ausubel, F.M., and Bolwell, G.P. (2012). The apoplastic oxidative burst peroxidase in Arabidopsis is a major component of pattern-triggered immunity. Plant Cell 24: 275–287.

Daudi, A., and O'Brien, J.A. (2012). Detection of hydrogen peroxide by DAB staining in Arabidopsis leaves. Bio. Protoc. 2: e263.

Dinasarapu, A.R., Saunders, B., Ozerlat, I., Azam, K., and Subramaniam, S. (2011). Signaling gateway molecule pages—A data model perspective. Bioinformatics 27: 1736–1738.

Dowler, S., Kular, G., and Alessi, D.R. (2002). Protein lipid overlay assay. Sci. STKE 2002: pl6.

Eyster, K.M. (2007). The membrane and lipids as integral participants in signal transduction: Lipid signal transduction for the non-lipid biochemist. Adv. Physiol. Educ. 31: 5–16.

Fang, C.T., Ken, H.C., Chen, T.Y., Chu, Y.K., Faan, H.C., and Wu, S.C. (1957). A comparison of the bice bacterial leaf blight organism with the bacterial leaf streak organisms of rice and Leersia hexandra Swartz. Acta Phytophysiol. Sin. 3: 99–124.

Ferjani, A., Segami, S., Horiguchi, G., Muto, Y., Maeshima, M., and Tsukaya, H. (2011). Keep an eye on PPi: The vacuolar-type H$^+$-pyrophosphatase regulates postgerminative development in Arabidopsis. Plant Cell 23: 2895–2908.

Fu, Z.Q., and Dong, X. (2013). Systemic acquired resistance: Turning local infection into global defense. Annu. Rev. Plant Biol. 64: 839–863.

Gerth, K., Lin, F., Menzel, W., Krishnamoorthy, P., Stenzel, I., Heilmann, M., and Heilmann, I. (2017). Guilt by association: A phenotype-based view of the plant phosphoinositide network. Annu. Rev. Plant Biol. 68: 349–374.

Guzel Deger, A., Scherzer, S., Nuhkat, M., Kedzierska, J., Kollist, H., Brosche, M., Unyayar, S., Boudsocq, M., Hedrich, R., and Roelfsema, M.R. (2015). Guard cell SLAC1-type anion channels mediate flagellin-induced stomatal closure. New Phytol. 208: 162–173.

Han, X., Yang, Y., Zhao, F., Zhang, T., and Yu, X. (2020). An improved protein lipid overlay assay for studying lipid-protein interactions. Plant Methods 16: 33.

Harper, S., and Speicher, D.W. (2011). Purification of proteins fused to glutathione S-transferase. Methods Mol. Biol. 681: 259–280.

Hasan, F., Shah, A.A., and Hameed, A. (2006). Industrial applications of microbial lipases. Enzyme Microb. Technol. 39: 235–251.

Hasegawa, J., Strunk, B.S., and Weisman, L.S. (2017). PI5P and PI(3,5)P$_2$: Minor, but essential phosphoinositides. Cell Struct. Funct. 42: 49–60.

Heilmann, I. (2016). Phosphoinositide signaling in plant development. Development 143: 2044–2055.

Hu, Y., Ding, Y., Cai, B., Qin, X., Wu, J., Yuan, M., Wan, S., Zhao, Y., and Xin, X.F. (2022). Bacterial effectors manipulate plant abscisic acid signaling for creation of an aqueous apoplast. Cell Host Microbe 30: 518–529.

Ichihara, A., Shiraishi, K., Sato, H., Sakamura, S., Nishiyama, K., Sakai, R., Furusaki, A., and Matsumoto, T. (1977). The structure of coronatine. J. Am. Chem. Soc. 99: 636–637.

Ji, Z., Ji, C., Liu, B., Zou, L., Chen, G., and Yang, B. (2016). Interfering TAL effectors of Xanthomonas oryzae neutralize R-gene-mediated plant disease resistance. Nat. Commun. 7: 1–9.

Joyce, P., Whitby, C.P., and Prestidge, C.A. (2016). Interfacial processes that modulate the kinetics of lipase-mediated catalysis using porous silica host particles. RSC Adv. 6: 43802–43813.

Kadota, Y., Sklenar, J., Derbyshire, P., Stransfeld, L., Asai, S., Ntoukakis, V., Jones, J.D., Shirasu, K., Menke, F., Jones, A., and Zipfel, C. (2014). Direct regulation of the NADPH oxidase RBOHD by the PRR-associated kinase BIK1 during plant immunity. Mol. Cell 54: 43–55.

Khush, G.S. (2005). What it will take to feed 5.0 billion rice consumers in 2030. Plant Mol. Biol. 59: 1–6.

Kriegel, A., Andres, Z., Medzihradszky, A., Kruger, F., Scholl, S., Delang, S., Patir-Nebioglu, M.G., Gute, G., Yang, H., Murphy, A.S., Peer, W.A., Pfeiffer, A., Krebs, M., Lohmann, J.U., and Schumacher, K. (2015). Job sharing in the endomembrane system: Vacuolar acidification requires the combined activity of V-ATPase and V-PPase. Plant Cell 27: 3383–3396.

Lawson, T., and Blatt, M.R. (2014). Stomatal size, speed, and responsiveness impact on photosynthesis and water use efficiency. Plant Physiol. 164: 1556–1570.

Leslie, M.E., and Heese, A. (2014). A re-elicitation assay to correlate flg22-signaling competency with ligand-induced endocytic degradation of the FLS2 receptor. Methods Mol. Biol. 1209: 149–162.

Li, L., Li, M., Yu, L., Zhou, Z., Liang, X., Liu, Z., Cai, G., Gao, L., Zhang, X., Wang, Y., Chen, S., and Zhou, J.M. (2014). The FLS2-associated kinase BIK1 directly phosphorylates the NADPH oxidase RbohD to control plant immunity. Cell Host Microbe **15:** 329–338.

Li, S.C., Diakov, T.T., Xu, T., Tarsio, M., Zhu, W., Couoh-Cardel, S., Weisman, L.S., and Kane, P.M. (2014). The signaling lipid PI(3,5)P$_2$ stabilizes V$_1$–V$_0$ sector interactions and activates the V-ATPase. Mol. Biol. Cell **25:** 1251–1262.

Logemann, E., Birkenbihl, R.P., Ülker, B., and Somssich, I.E. (2006). An improved method for preparing *Agrobacterium* cells that simplifies the *Arabidopsis* transformation protocol. Plant Methods **2:** 1–5.

Lozano-Duran, R., Bourdais, G., He, S.Y., and Robatzek, S. (2014). The bacterial effector HopM1 suppresses PAMP-triggered oxidative burst and stomatal immunity. New Phytol. **202:** 259–269.

Maeshima, M., and Yoshida, S. (1989). Purification and properties of vacuolar membrane proton-translocating inorganic pyrophosphatase from mung bean. J. Biol. Chem. **264:** 20068–20073.

Margets, A., Rima, S., Helm, M., and Carter, M. (2021). Molecular mechanism and structure-zooming in on plant immunity. Mol. Plant Microbe. Interact. **34:** 1346–1349.

McCartney, A.J., Zhang, Y., and Weisman, L.S. (2014). Phosphatidylinositol 3,5-bisphosphate: Low abundance, high significance. BioEssays **36:** 52–64.

McLachlan, D.H., Kopischke, M., and Robatzek, S. (2014). Gate control: Guard cell regulation by microbial stress. New Phytol. **203:** 1049–1063.

Melotto, M., Underwood, W., Koczan, J., Nomura, K., and He, S.Y. (2006). Plant stomata function in innate immunity against bacterial invasion. Cell **126:** 969–980.

Morishita, M., Morimoto, F., Kitamura, K., Koga, T., Fukui, Y., Maekawa, H., Yamashita, I., and Shimoda, C. (2002). Phosphatidylinositol 3-phosphate 5-kinase is required for the cellular response to nutritional starvation and mating pheromone signals in *Schizosaccharomyces pombe*. Genes Cells **7:** 199–215.

Niño-Liu, D.O., Ronald, P.C., and Bogdanove, A. (2006). *Xanthomonas oryzae* pathovars: Model pathogens of a model crop. Mol. Plant Pathol. **7:** 303–324.

Notti, R.Q., and Stebbins, C.E. (2016). The structure and function of type III secretion systems. Microbiol. Spectr. **4:** 241–264.

Nováková, P., Hirsch, S., Feraru, E., Tejos, R., van Wijk, R., Viaene, T., Heilmann, M., Lerche, J., De Rycke, R., Feraru, M.I., Grones, P., Montagu, M.V., Heilmann, I., Munnik, T., and Friml, J. (2014). SAC phosphoinositide phosphatases at the tonoplast mediate vacuolar function in *Arabidopsis*. Proc. Natl. Acad. Sci. U.S.A. **111:** 2818–2823.

Perez Koldenkova, V., and Hatsugai, N. (2017). Vacuolar convolution: Possible mechanisms and role of phosphatidylinositol 3,5-bisphosphate. Funct. Plant Biol. **44:** 751–760.

Sato, H., Frank, D.W., Hillard, C.J., Feix, J.B., Pankhaniya, R.R., Moriyama, K., Finck-Barbançon, V., Buchaklian, A., Lei, M., Long, R.M., Wiener-Kronish, J., and Sawa, T. (2003). The mechanism of action of the *Pseudomonas aeruginosa*-encoded type III cytotoxin, ExoU. EMBO J. **22:** 2959–2969.

Scholz-Starke, J. (2017). How may PI(3,5)P$_2$ impact on vacuolar acidification? Channels (Austin) **11:** 497–498.

Segami, S., Asaoka, M., Kinoshita, S., Fukuda, M., Nakanishi, Y., and Maeshima, M. (2018). Biochemical, structural and physiological characteristics of vacuolar H$^+$-pyrophosphatase. Plant Cell Physiol. **59:** 1300–1308.

Spiegel, S., Foster, D., and Kolesnick, R. (1996). Signal transduction through lipid second messengers. Curr. Opin. Cell Biol. **8:** 159–167.

Svendsen, A. (2000). Lipase protein engineering. Biochim. Biophys. Acta **1543:** 223–238.

Swings, J., Van den Mooter, M., Vauterin, L., Hoste, B., Gillis, M., Mew, T., and Kersters, K. (1990). Reclassification of the causal agents of bacterial blight (*Xanthomonas campestris* pv. *oryzae*) and bacterial leaf streak (*Xanthomonas campestris* pv. *oryzicola*) of rice as pathovars of *Xanthomonas oryzae* (ex Ishiyama 1922) sp. nov., nom. rev. Int. J. Syst. Evol. Microbiol. **40:** 309–311.

Thor, K., Jiang, S., Michard, E., George, J., Scherzer, S., Huang, S., Dindas, J., Derbyshire, P., Leitão, N., DeFalco, T.A., Köster, P., Hunter, K., Kimura, S., Gronnier, J., Stransfeld, L., Kadota, Y., Bücherl, C.A., Charpentier, M., Wrzaczek, M., MacLean, D., Oldroyd, G.E.D., Menke, F.L.H., Roelfsema, M.R.G., Hedrich, R., Feijó, J., and Zipfel, C. (2020). The calcium-permeable channel OSCA1.3 regulates plant stomatal immunity. Nature **585:** 569–573.

Van Meer, G., Voelker, D.R., and Feigenson, G.W. (2008). Membrane lipids: Where they are and how they behave. Nat. Rev. Mol. Cell Biol. **9:** 112–124.

Voelker, C., Schmidt, D., Mueller-Roeber, B., and Czempinski, K. (2006). Members of the *Arabidopsis* AtTPK/KCO family form homomeric vacuolar channels in planta. Plant J. **48:** 296–306.

Wang, S., Li, S., Wang, J., Li, Q., Xin, X.F., Zhou, S., Wang, Y., Li, D., Xu, J., Luo, Z.Q., He, S.Y., and Sun, W. (2021). A bacterial kinase phosphorylates OSK1 to suppress stomatal immunity in rice. Nat. Commun. **12:** 5479.

Xu, X., Xu, Z., Li, Z., Zakria, M., Zou, L., and Chen, G. (2021). Increasing resistance to bacterial leaf streak in rice by editing the promoter of susceptibility gene OsSULRT3; 6. Plant Biotechnol. J. **19:** 1101–1103.

Ye, W., and Murata, Y. (2016). Microbe associated molecular pattern signaling in guard cells. Front. Plant Sci. **7:** 583.

Yekondi, S., Liang, F.C., Okuma, E., Radziejwoski, A., Mai, H.W., Swain, S., Singh, P., Gauthier, M., Chien, H.C., Murata, Y., and Zimmerli, L. (2018). Nonredundant functions of *Arabidopsis* LecRK-V.2 and LecRK-VII.1 in controlling stomatal immunity and jasmonate-mediated stomatal closure. New Phytol. **218:** 253–268.

Yuan, M., Jiang, Z., Bi, G., Nomura, K., Liu, M., Wang, Y., Cai, B., Zhou, J.M., He, S.Y., and Xin, X.F. (2021). Pattern-recognition receptors are required for NLR-mediated plant immunity. Nature **592:** 105–109.

Zamora, O., Schulze, S., Azoulay-Shemer, T., Parik, H., Unt, J., Brosche, M., Schroeder, J.I., Yarmolinsky, D., and Kollist, H. (2021). Jasmonic acid and salicylic acid play minor roles in stomatal regulation by CO$_2$, abscisic acid, darkness, vapor pressure deficit and ozone. Plant J. **108:** 134–150.

Zeng, W., and He, S.Y. (2010). A prominent role of the flagellin receptor FLAGELLIN-SENSING2 in mediating stomatal response to *Pseudomonas syringae* pv. *tomato* DC3000 in *Arabidopsis*. Plant Physiol. **153:** 1188–1198.

Zhang, M., Wang, Y., Chen, X., Xu, F., Ding, M., Ye, W., Kawai, Y., Toda, Y., Hayashi, Y., Suzuki, T., Zeng, H., Xiao, L., Xiao, X., Xu, J., Guo, S., Yan, F., Shen, Q., Xu, G., Kinoshita, T., and Zhu, Y. (2021). Plasma membrane H($^+$)-ATPase overexpression increases rice yield via simultaneous enhancement of nutrient uptake and photosynthesis. Nat. Commun. **12:** 735.

Zhang, W., He, S.Y., and Assmann, S.M. (2008). The plant innate immunity response in stomatal guard cells invokes G-protein-dependent ion channel regulation. Plant J. **56:** 984–996.

Zou, L.F., Li, Y.R., and Chen, G.Y. (2011). A non-marker mutagenesis strategy to generate poly-*hrp* gene mutants in the rice pathogen *Xanthomonas oryzae* pv. *oryzicola*. Agric. Sci. China **10:** 1139–1150.

Zou, L., Wang, X., Xiang, Y., Zhang, B., Li, Y., Xiao, Y., Wang, J., Walmsley, A.R., and Chen, G. (2006). Elucidation of the *hrp* clusters of *Xanthomonas oryzae* pv. *oryzicola* that control the hypersensitive response in nonhost tobacco and pathogenicity in susceptible host rice. Appl. Environ. Microbiol. **72:** 6212–6224.

Zou, M., Guo, M., Zhou, Z., Wang, B., Pan, Q., Li, J., Zhou, J.M., and Li, J. (2021). MPK3- and MPK6-mediated VLN3 phosphorylation regulates

actin dynamics during stomatal immunity in *Arabidopsis*. Nat. Commun. **12**: 6474.

SUPPORTING INFORMATION

Additional Supporting Information may be found online in the supporting information tab for this article: http://onlinelibrary.wiley.com/doi/10.1111/jipb.13344/suppinfo

Scan using WeChat with your
smartphone to view JIPB online

Scan with iPhone or iPad to
view JIPB online